COMBINED EFFECTS ON MHD FREE CONVECTION THREE DIMENSIONAL FLOW THROUGH POROUS MEDIUM IN VERTICAL PLATES

L. HARI KRISHNA, M. VEERA KRISHNA

Abstract: The effects of radiation and hall current on MHD free convection three dimensional flow in a vertical channel filled with porous medium has been studied. We consider an incompressible viscous and electrically conducting incompressible viscous fluid in a parallel plate channel bounded by a loosely packed porous medium. The fluid is driven by a uniform pressure gradient parallel to the channel plates and the entire flow field is subjected to a uniform inclined magnetic field of strength H_o inclined at an angle of inclination α with the normal to the boundaries in the transverse *xy*-plane. The temperature of one of the plates varies periodically and the temperature difference of the plates is high enough to induce radiative heat transfer. The effects of various parameters on the velocity profiles, the skin friction, temperature field, rate of heat transfer in terms of their amplitude and phase angles are shown graphically.

Keywords: steady hydro magnetic flows, three dimensional flows, parallel plate channel, porous medium, radiative heat transfer, optically thin fluid.

Introduction: The flow of fluids through porous media are encountered in a wide range of engineering and industrial applications such as in recovery or extraction of crude oil, geothermal systems, thermal insulation, heat exchangers, storage of nuclear wastes, packed bed catalytic reactors, atmospheric and oceanic circulations. Several scholars viz. Crammer and Pai [1], Ferraro and Plumpton [2], Shercliff [3] have studied such flows because of their varied importance. MHD channel or duct flows are important from its practical point of view. Chang and Lundgren [4] have studied a hydro magnetic flow in a duct. Yen and Chang [5] analysed the effect of wall electrical conductance onthe magneto hydro dynamic Couette flow. From the technological point of view and due to practical applications, free convective flow and heat transfer problems are always important. This process of heat transfer is encountered in cooling of nuclear reactors, providing heat sinks in turbine blades and aeronautics. Ostrach [6] studied the combined effects of natural and forced convection laminar flow and heat transfer of fluids with and without heat sources in channels with linearly varying wall temperature. Jain and Gupta [7] studied three dimensional free convection Couette flow with transpiration cooling There are numerous important engineering and geophysical applications of the channel flows through porous medium, for example in the fields of agricultural engineering for channel irrigation and to study the underground water resources, in petroleum technology to study the movement of natural gas, oil and water through the oil channels/reservoirs. Transient natural convection between two vertical walls with a porous material having variable porosity has been studied by Paul *et al*[8]. Sahin [9] investigated the three-dimensional free convective channel flow through porous medium. In recent years, the effects of transversely applied magnetic field on the flows of electrically conducting viscous fluids have been discussed widely owing to their astrophysics, geophysical and engineering applications. Attia and Kotb [10] studied MHD flow between two parallel plates with heat transfer. When the strength of the magnetic field is strong, one cannot neglect the effects of Hall current. The rotating flow of an electrically conducting fluid in the presence of a magnetic field is encountered in geophysical and cosmical fluid dynamics. It is also important in the solar physics involved in the sunspot development. Soundalgekar [11] studied the Hall effects in MHD Couette flow with heat transfer.

2. Formulation and Solution of the Problem:

Consider an unsteady MHD free convective flow of an electrically conducting, viscous, incompressible fluid through a porous medium bounded between two insulated infinite vertical plates in the presence of Hall current and thermal radiation. The plates are at a distance *d* apart. A Cartesian coordinate system with *x*-axis oriented vertically upward along the centre line of the channel is introduced. The *z*-axis is taken perpendicular to the planes of the plates as shown in Fig. 1.

We choose a Cartesian system O(*x, y, z*) such that the boundary walls are at *z*=0 and *z*=*l* and are assumed to be parallel to *xy*-plane. The steady flow through porous medium is governed by Brinkman's equations. At the interface the fluid satisfies the continuity condition of velocity and stress. The boundary plates are assumed to be parallel to *xy*-plane and the

magnetic field of strength H_o inclined at an angle of inclination α to the z-axis in the transverse xz-plane.

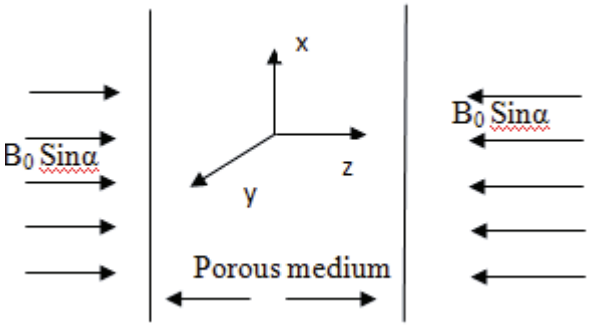

Fig. 1 Physical Configuration of the Problem

The component along z-direction induces a secondary flow in that direction while its x-components changes perturbation to the axial flow. The steady hydro magnetic equations governing the incompressible fluid under the influence of a uniform inclined magnetic field of strength H_o inclined at an angle of inclination α with reference to a frame are

$$\frac{\partial u}{\partial t} = -\frac{1}{\rho}\frac{\partial p}{\partial x} + \nu\frac{\partial^2 u}{\partial z^2} - \frac{\mu_e J_z H_0 Sin\alpha}{\rho} - \frac{\nu}{k}u + g\beta T \tag{2.1}$$

$$\frac{\partial w}{\partial t} = \nu\frac{\partial^2 w}{\partial z^2} + \frac{\mu_e J_x H_0 Sin\alpha}{\rho} - \frac{\nu}{k}w \tag{2.2}$$

Where, All the physical quantities in the above equation have their usual meaning. (*u, w*) are the velocity components along O(*x, z*) directions respectively. ρ is the density of the fluid, μ_e is the magnetic permeability, ν is the coefficient of kinematic viscosity, *k* is the permeability of the medium, H_o is the applied magnetic field. When the strength of the magnetic field is very large, the generalized Ohm's law is modified to include the Hall current, so that

$$J + \frac{\omega_e \tau_e}{H_0} J \times H = \sigma\,(E + \mu_e\, q \times H) \tag{2.3}$$

Where, ***q*** is the velocity vector, H is the magnetic field intensity vector, E is the electric field , J is the current density vector, ω_e is the cyclotron frequency, τ_e is the electron collision time, σ is the fluid conductivity and, μ_e is the magnetic permeability. In equation (2.3) the electron pressure gradient, the ion-slip and thermo-electric effects are neglected. We also assume that the electric field *E*=0 under assumptions reduces to

$$J_x - m\,J_z Sin\alpha = -\sigma\mu_e H_0 w\, Sin\alpha \tag{2.4}$$

$$J_z + m\,J_x Sin\alpha = -\sigma\mu_e H_0 u Sin\alpha \tag{2.5}$$

Where $m = \omega_e\tau_e$ is the hall parameter.

On solving equations (2.3) and (2.4) we obtain

$$J_x = \frac{\sigma\mu_e H_0 Sin\alpha}{1 + m^2 Sin^2\alpha}(umSin\alpha - w) \tag{2.6}$$

$$J_z = \frac{\sigma\mu_e H_0 Sin\alpha}{1 + m^2 Sin^2\alpha}(u + w\,mSin\alpha) \tag{2.7}$$

Using the equations (2.6.) and (2.7), the equations of the motion with reference to frame are given by

$$\frac{\partial u}{\partial t} = -\frac{1}{\rho}\frac{\partial p}{\partial x} + \nu\frac{\partial^2 u}{\partial z^2} - \frac{\sigma\mu_e{}^2 H_0{}^2 Sin\alpha}{\rho(1 + m^2 Sin^2\alpha)}(u + w\,mSin\alpha) - \frac{\nu}{k}u + g\beta T \tag{2.8}$$

$$\frac{\partial w}{\partial t} = \nu\frac{\partial^2 w}{\partial z^2} + \frac{\sigma\mu_e{}^2 H_0{}^2 Sin\alpha}{\rho(1 + m^2 Sin^2\alpha)}(umSin\alpha - w) - \frac{\nu}{k}w \tag{2.9}$$

$$\rho C_p\frac{\partial T}{\partial t} = K\frac{\partial^2 T}{\partial z^2} - \frac{\partial q}{\partial z} \tag{2.10}$$

The boundary conditions for the problem are

$$u = w = T = 0, \quad z = -\frac{d}{2} \tag{2.11}$$

$$u = w = 0, T = T_w Cos\,\omega t, \qquad z = \frac{d}{2} \tag{2.12}$$

Where T_w is the mean temperature of the plate at z=d/2 and ω is the frequency of oscillations. Following Cogley et.al [22], the last term in the energy equation (2.10),

$$\frac{\partial q}{\partial z} = 4\alpha^2(T - T_0)$$

Stands for radiative heat flux modifies to

$$\frac{\partial q}{\partial z} = 4\alpha^2 T \tag{2.13}$$

in view of the reference temperature $T_0 = 0$, where is mean radiation absorption co-efficient.

We introduce the following non-dimensional variables and parameters.

$$z^* = \frac{z}{d},\ x = \frac{x}{d}, u = \frac{u^*}{U}, v = \frac{v^*}{U},\ q = \frac{q^*}{U},\ t^* = \frac{tU}{d},$$

$$\omega^* = \frac{\omega d}{U}\ p^* = \frac{p}{\rho U^2},\ T^* = \frac{T}{T_w}$$

Where, U is the mean axial velocity,

Making use of non-dimensional variables, the governing equations reduces to (dropping asterisks),

$$\frac{\partial u}{\partial t} = -\frac{\partial p}{\partial x} + \frac{1}{\mathrm{Re}}\frac{\partial^2 u}{\partial z^2} - \frac{M^2 Sin^2\alpha}{Re(1 + m^2 Sin^2\alpha)}(u + wmSin\alpha) - \frac{D^{-1}}{Re}u - GrT \tag{2.14}$$

$$\frac{\partial w}{\partial t} = \frac{1}{\mathrm{Re}}\frac{\partial^2 w}{\partial z^2} + \frac{M^2 Sin^2\alpha}{Re(1+m^2 Sin^2\alpha)}(umSin\alpha - w) - \frac{D^{-1}}{Re}w \quad (2.15)$$

$$\frac{\partial T}{\partial t} = \frac{1}{Pe}\frac{\partial^2 T}{\partial z^2} - \frac{R^2}{Pe}\frac{\partial q}{\partial z} \quad (2.16)$$

Where, $\mathrm{Re} = \frac{Ud}{\nu}$ is the Reynolds number

$D = \frac{K}{d^2}$ the permeability parameter (Darcy parameter), $Gr = \frac{g\beta d^2 T}{\nu U}_w$ the Grashoff number

$Pe = \frac{\rho C_p dU}{\nu U}$ the Peclet number , $R = \frac{2\alpha d}{\sqrt{K}}$ the radiation parameter

The corresponding transformed boundary conditions are

$$u = w = T = 0, \quad z = -\frac{1}{2} \quad (2.18)$$

$$u = w = 0, T = Cos\,\omega t, \qquad z = \frac{1}{2} \quad (2.19)$$

For the oscillatory internal flow, we shall assume that the fluid flows only under the influence of a non-dimensional pressure gradient oscillating in the in the direction of *x*-axis only which is of the form,

$$-\frac{\partial p}{\partial x} = P\,Cos\,\omega t \quad (2.20)$$

In order to combine equations (2.14) and (2.15) into single equation, we introduce a complex function $F = u + iw$ and using equation (2.22), we obtain

$$\mathrm{Re}\frac{\partial q}{\partial t} = -P\,Cos\,\omega t + \frac{\partial^2 q}{\partial z^2} - \left(\frac{M^2 Sin^2\alpha}{(1-imSin\alpha)} + i\omega\,\mathrm{Re} + D^{-1}\right)q - GrT \quad (2.21)$$

The boundary conditions in complex form are

$$q = T = 0, \quad z = -\frac{1}{2} \quad (2.22)$$

$$q = 0, T = e^{i\omega t}, \qquad z = \frac{1}{2} \quad (2.23)$$

In order to solve the equations (2.16) and (2.21) making use of boundary conditions (2.22) and (2.23), we assume in the complex form the solution of the problem as

$$q(z,t) = q_0(z)e^{i\omega t},\ T(z,t) = \theta_0(z)e^{i\omega t},\ -\frac{\partial p}{\partial x} = P\,e^{i\omega t} \quad (2.24)$$

Substituting equations (2.24) in equations (2.16) and (2.21), we get

$$\frac{d^2 q_0}{dz^2} - \lambda^2 q_0 = -P\,\mathrm{Re} - Gr\,\theta_0 \quad (2.24)$$

and

$$\frac{d^2 q_0}{dz^2} - \xi^2\theta_0 = 0 \quad (2.25)$$

Where, $\lambda^2 = \frac{M^2 Sin^2\alpha}{(1-imSin\alpha)} + i\omega\,\mathrm{Re} + D^{-1}$ and $\xi^2 = i\omega Pe + R^2$

The boundary conditions given in equations (2.22) and (2.23) become

$$q_0 = \theta_0 = 0, \quad z = -\frac{1}{2} \quad (2.26)$$

$$q_0 = 0, \theta_0 = 1, \quad z = \frac{1}{2} \quad (2.27)$$

The ordinary differential equations (2.24) and (2.25) are solved under the boundary conditions given in equations (2.26) and (2.27) for the velocity and temperature fields. The solution of the problem is obtained as

$$q(z,t) = \left\{\frac{P\,\mathrm{Re}}{\lambda^2}\left(1 - \frac{Cosh\lambda z}{Cosh\frac{\lambda}{2}}\right) + \frac{Gr}{\lambda^2 - \xi^2}\left(\frac{Sinh\lambda\left(z+\frac{1}{2}\right)}{Sinh\lambda} - \frac{Sinh\xi\left(z+\frac{1}{2}\right)}{Sinh\xi}\right)\right\}e^{i\omega t} \quad (2.28)$$

$$T(z,t) = \frac{Sinh\xi\left(z+\frac{1}{2}\right)}{Sinh\xi}\,e^{i\omega t} \quad (2.29)$$

Now from the velocity field, we can obtain the skin-friction at the left plate in terms of its amplitude and phase angle as

$$\tau_L = \left(\frac{\partial q}{\partial z}\right)_{z=-1/2} = \left(\frac{\partial q_0}{\partial z}\right)_{z=-1/2} e^{i\omega t} = |q|\,Cos(\omega t + \phi)$$

Where $|q| = \sqrt{(\mathrm{Re}\,q)^2 + (\mathrm{Im}\,q)^2}$ and $\phi = Tan^{-1}\left(\frac{\mathrm{Re}\,q}{\mathrm{Im}\,q}\right)$

$$\mathrm{Re}\,q + i\,\mathrm{Im}\,q = \frac{P\,\mathrm{Re}}{\lambda^2}Tanh\left(\frac{\lambda}{2}\right) + \frac{Gr}{\lambda^2 - \xi^2}\left[\frac{\lambda}{Sinh\lambda} - \frac{\xi}{Sinh\xi}\right] \quad (2.30)$$

From the temperature field, the rate of heat transfer *Nu* (Nusselt number) at the left plate in terms of its amplitude and phase angle is obtained

$$Nu = \left(\frac{\partial T}{\partial z}\right)_{z=-1/2} = \left(\frac{\partial \theta_0}{\partial z}\right)_{z=-1/2} e^{i\omega t} = |H|\,Cos(\omega t + \psi) \quad (2.31)$$

Where $|H| = \sqrt{(\mathrm{Re}\,H)^2 + (\mathrm{Im}\,H)^2}$,

$\psi = Tan^{-1}\left(\frac{\mathrm{Re}\,H}{\mathrm{Im}\,H}\right)$ and $\mathrm{Re}\,H + i\,\mathrm{Im}\,H = \frac{\xi}{Sinh\xi}$

3. Results and Discussion: The computational results are presented in Figures (2-19) for the velocity profiles (fixing $\alpha = \pi/3$), Figures (20-22) for temperature profiles and Figures (24-26) for amplitude and phase angle of rate of heat tranfer with respect to different governing parameters and also tables (1-2) for shear stresses and rate of heat transfer at z = -1/2. We noticed that, from Figures (2 & 3) shows the variation of velocity profiles under the influence of the Reynolds parameter *Re*. The magnitude of the velocity *u* increases and *w* decreases with increase in Raynolds number *R*. It is evident from that increasing value of *R*e leads to the increase of resultant velocity. It is interesting to note that from figures (4 & 5) both the magnitude of velocity components *u* and *w* decreases with the increase of intensity of the magnetic field (Hartmann number *M*). This is because of the reason that effect of a inclined magnetic field on an electrically conducting fluid gives rise to a resistive type force (called Lorentz force) similar to drag force and upon increasing the values of *M* increases the drag force which has tendency to slow down the motion of the fluid. The resultant velocity also reduces with increase in the intensity of the magnetic field. The magnitudes of the velocity components *u* and *w* increase with the increase in permeability of the porous medium (*D*) is observed from Figures (6 & 7). Lower the permeability of the porous medium lesser the fluid speed is in the entire fluid region. It is expected physically also because the resistance posed by the porous medium to the decelerated flow due to inclined magnetic field reduces with decreasing permeability *D* which leads to decrease in the velocity. The resultant velocity also increases with increase in *D*. The variation of the velocity profiles with hall parameter *m* is shown in Figures (8 & 9). The magnitudes of the velocity components *u*, *w* and the resultant velocity increases with the increase of hall parameter *m* throughout the channel and there is no significant effect of hall parameter *m* on both the velocity components with the effect of inclined magnetic field. The variations of the velocity profiles with the Grashof number *Gr* are shown in Figures (10 & 11). The magnitude of the velocity components *u* enhances & *w* decreases with the increasing Grashof number *Gr*. The maximum of the velocity profiles shifts towards right half of the channel due to the greater buoyancy force in this part of the channel due to the presence of hotter plate. In the right half there lies hot plate at z = 1/2 and heat is transferred from the hot plate to the fluid and consequently buoyancy force enhances the flow velocity further. In the left half of the channel, the transfer of heat takes place from the fluid to the cooler plate at z = –1/2. Thus, the effect of Grashof number on the resultant velocity is reversed i.e. velocity decreases with increasing *Gr*. The velocity profiles with the Peclet number *Pe* are shown in Figures (12 & 13). The magnitude of the velocity components *u* enhances & *w* decreases with the increasing Peclet number *Pe*. We noticed that with increasing Peclet number *P*e the resultant velocity decreases. The variation of velocity profile with radiation parameter *R* is shown in Figures (14 & 15). The magnitude of velocity components *u* and *w* decrease with increasing in Radiation parameter *R*. In the left half of the channel, the effect of *R* on velocity is insignificant while in the right half of the channel velocity decreases with increase of *R*. It is evident from the Figures (16 & 17) that, the velocity components *u* enhances *w* reduces with increase in pressure gradient *P*. The increasing pressure gradient *P* leads to the increase of resultant velocity. The velocity profiles with the frequency of oscillation ω are shown in Figures (18 & 19). The magnitude of the velocity component *u* enhances firstly and gradually decreases then experienced enhancement as observed with increase in the frequency of oscillation ω. Likewise the behaviour of the velocity component *w* experiences enhancement and then gradually decreases throughout the fluid region with increase in the frequency of oscillation ω. The resultant velocity decreases with increasing the frequency of oscillations ω.

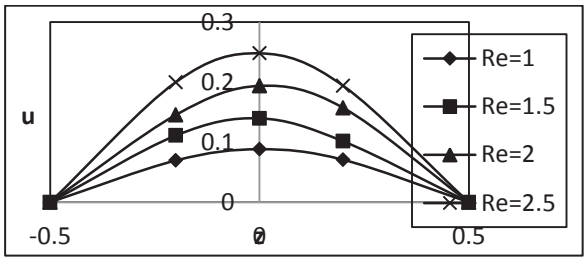

Fig. 2: The velocity Profile for u against Re with
$P=5, Pe=0.7, Gr=1, D=1, R=1, M=5, m=1, \omega=5, t=1$

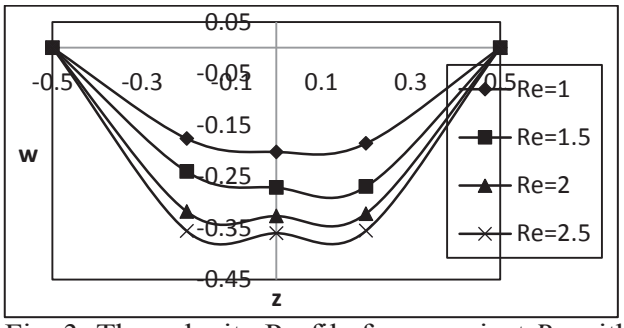

Fig. 3: The velocity Profile for w against Re with
$P=5, Pe=0.7, Gr=1, D=1, R=1, M=5, m=1, \omega=5, t=1$

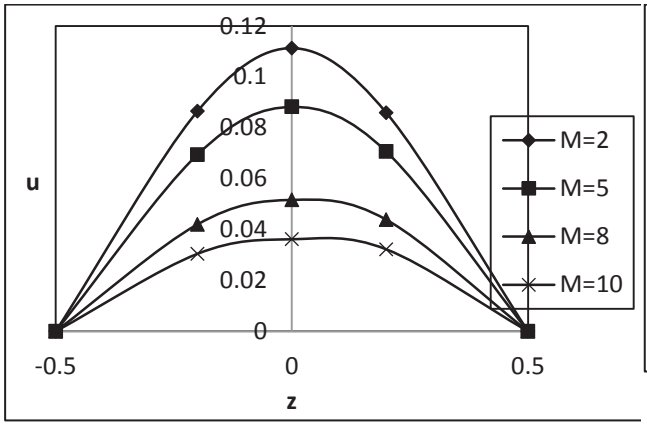

Fig. 4: The velocity Profile for u against M with
$P=5, Pe=0.7, \mathrm{Re}=1, Gr=1, D=1, R=1, m=1, \omega=5, t=1$

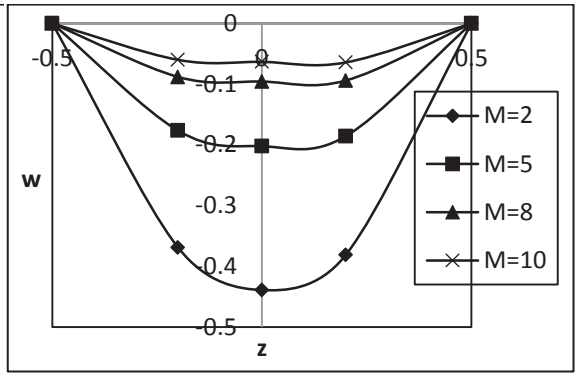

Fig. 5: The velocity Profile for w against M with
$P=5, Pe=0.7, \mathrm{Re}=1, Gr=1, D=1, R=1, m=1, \omega=5, t=1$

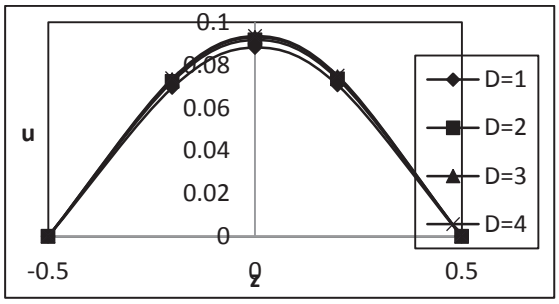

Fig. 6: The velocity Profile for u against D with
$P=5, Pe=0.7, \mathrm{Re}=1, Gr=1, R=1, M=5, m=1, \omega=5, t=1$

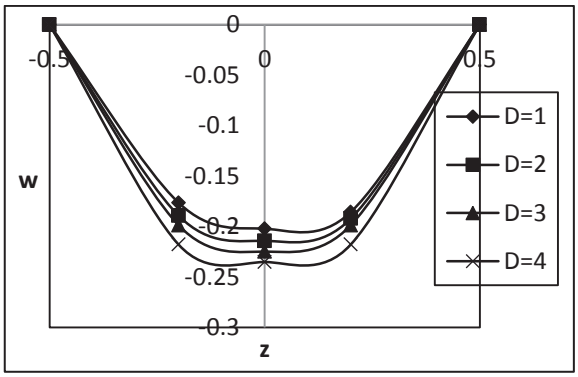

Fig. 7: The velocity Profile for w against D with
$P=5, Pe=0.7, \mathrm{Re}=1, Gr=1, R=1, M=5, m=1, \omega=5, t=1$

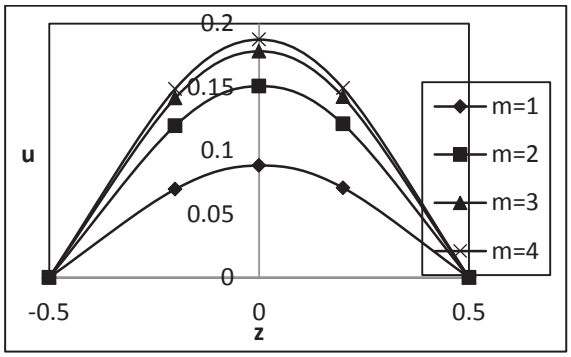

Fig. 8: The velocity Profile for u against m with
$P = 5, Pe = 0.7, \mathrm{Re} = 1,\ Gr = 1, D = 1, R = 1, M = 5,\ \omega = 5, t = 1$

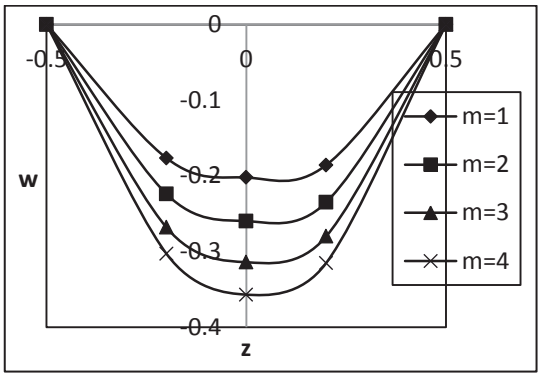

Fig. 9: The velocity Profile for w against m with
$P = 5, Pe = 0.7, \mathrm{Re} = 1,\ Gr = 1, D = 1, R = 1, M = 5,\ \omega = 5, t = 1$

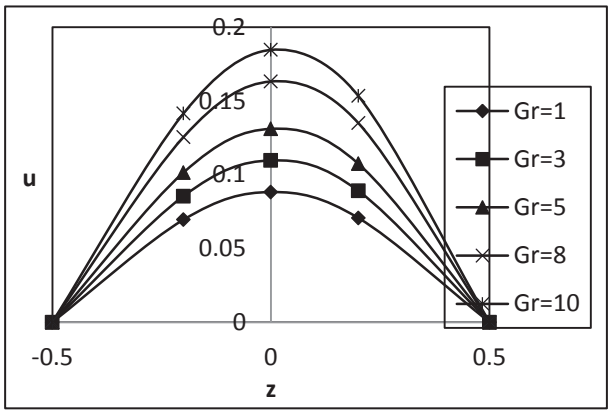

Fig. 10: The velocity Profile for u against Gr with
$P = 5, Pe = 0.7, \mathrm{Re} = 1,\ D = 1, R = 1, M = 5, m = 1,\ \omega = 5, t = 1$

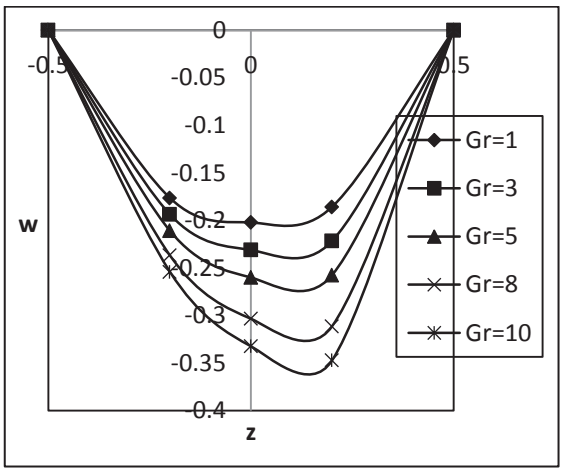

Fig. 11: The velocity Profile for w against Gr with
$P = 5, Pe = 0.7, \mathrm{Re} = 1,\ D = 1, R = 1, M = 5, m = 1,\ \omega = 5, t = 1$

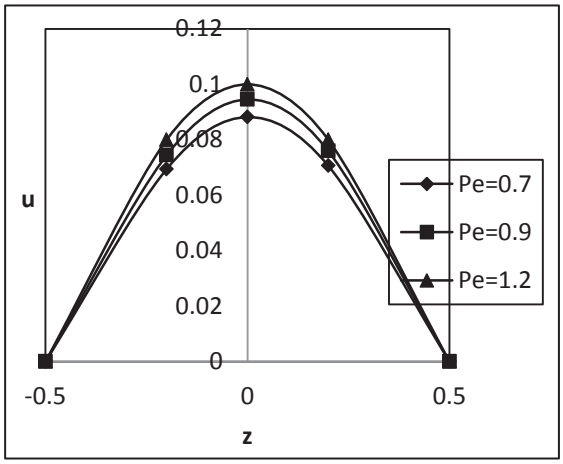

Fig. 12: The velocity Profile for u against Pe with
$P = 5,\ \mathrm{Re} = 1,\ Gr = 1, D = 1, R = 1, M = 5, m = 1,\ \omega = 5, t = 1$

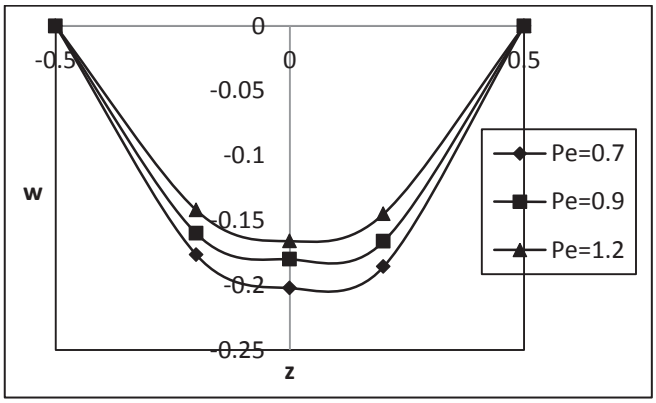

Fig. 13: The velocity Profile for w against Pe with
$P = 5,\ \mathrm{Re} = 1,\ Gr = 1, D = 1, R = 1, M = 5, m = 1,\ \omega = 5, t = 1$

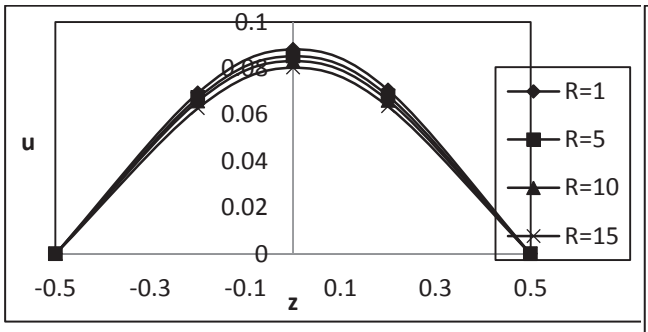

Fig. 14: The velocity Profile for u against R with
$P=5, Pe=0.7, \mathrm{Re}=1,\ Gr=1, D=1, M=5, m=1,\ \omega=5, t=1$

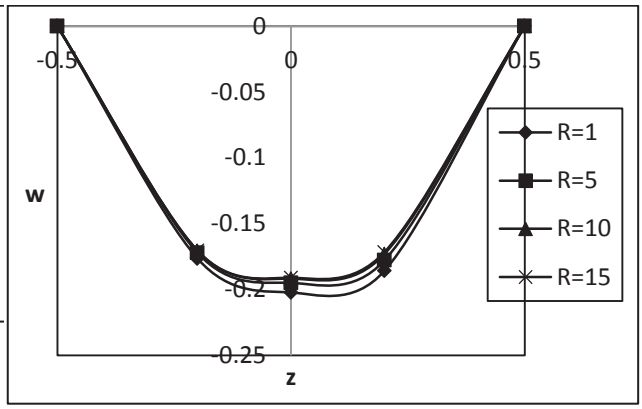

Fig. 15: The velocity Profile for w against R with
$P=5, Pe=0.7, \mathrm{Re}=1,\ Gr=1, D=1, M=5, m=1,\ \omega=5, t=1$

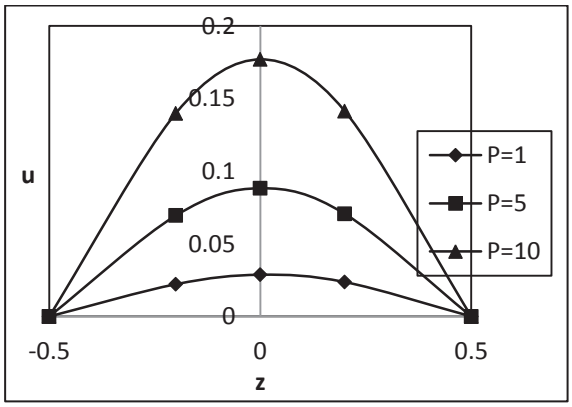

Fig. 16: The velocity Profile for u against P with
$Pe=0.7, \mathrm{Re}=1,\ Gr=1, D=1, R=1, M=5, m=1,\ \omega=5, t=1$

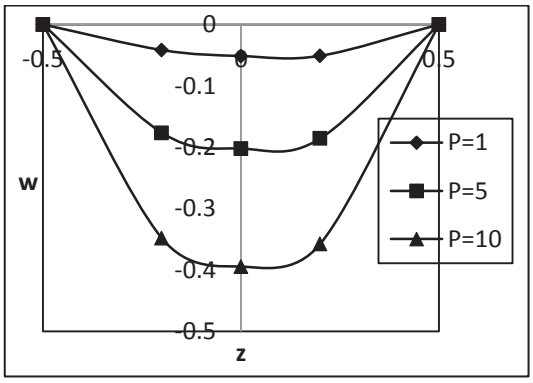

Fig. 17: The velocity Profile for w against P with
$Pe=0.7, \mathrm{Re}=1,\ Gr=1, D=1, R=1, M=5, m=1,\ \omega=5, t=1$

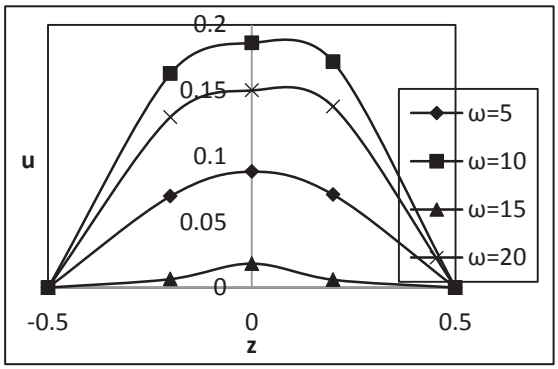

Fig. 18: The velocity Profile for u against ω with
$Pe=0.7, \mathrm{Re}=1,\ Gr=1, D=1, R=1, M=5, m=1,\ P=5, t=1$

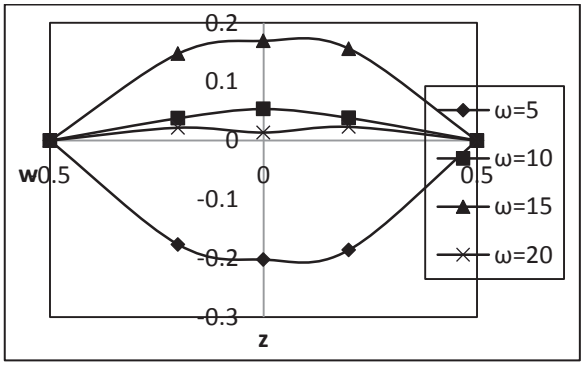

Fig. 19: The velocity Profile for w against ω with
$Pe=0.7, \mathrm{Re}=1,\ Gr=1, D=1, R=1, M=5, m=1,\ P=5, t=1$

The temperature profiles are shown in Figure (20-22). The temperature decreases with the increase of radiation parameter N, the Peclet number Pe (Figures 20-21). The temperature enhances initially and then gradually decreases with increase in the frequency of oscillations ω (Figure 22). We notice that the flow of heat tranfer is reversed with the increase in Peclet number Pe. The amplitude $|H|$ of the rate of heat transfer is shown in (Fig. 23 & 24) which shows that the value of $|H|$ decreases with the increase of

R and *Pe*. The phase angle ψ of the rate of heat transfer is shown in (Fig. 25 &26). It is noticed that phase angle ψ decreases with the increase in *Pe* and increases with increase in *R*. there is only phase log for the values of the frequency of oscillations ω.

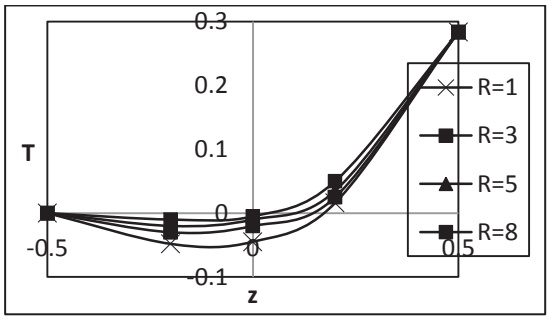

Fig. 20: TheTemperature Profile for *T*against *R* with $Pe = 0.7, \omega = 5, t = 1$

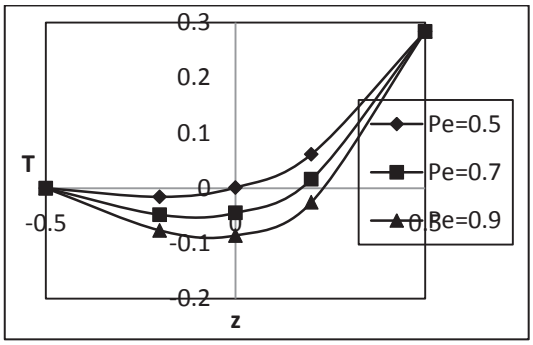

Fig. 21: The Temperature Profile for *T*against *Pe* with $R = 1,\ \omega = 5, t = 1$

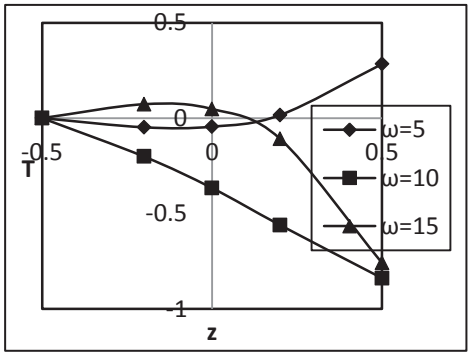

Fig.22: The Temperature Profile for *T*against ω with $Pe = 0.7, R = 1,\ t = 1$

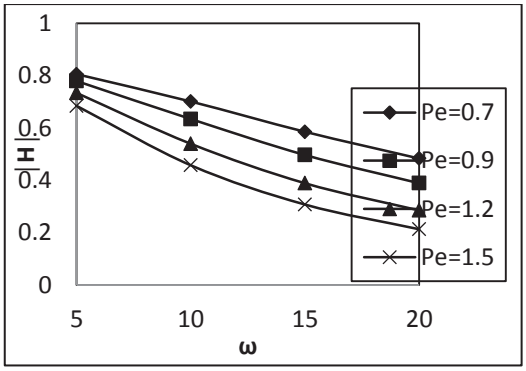

Fig. 23: Amplitude $(|H|)$of Rate of Heat transfer profile against *Pe* with R=1

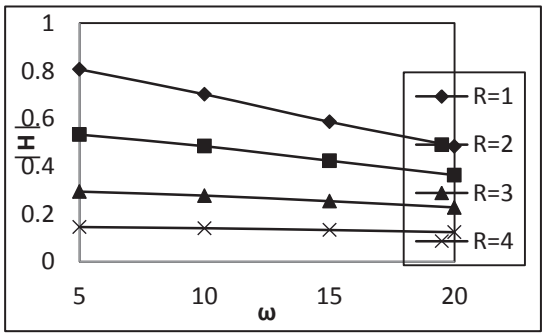

Fig. 24: Amplitude $(|H|)$ of Rate of Heat transfer profile against *R* with *Pe*=0.7

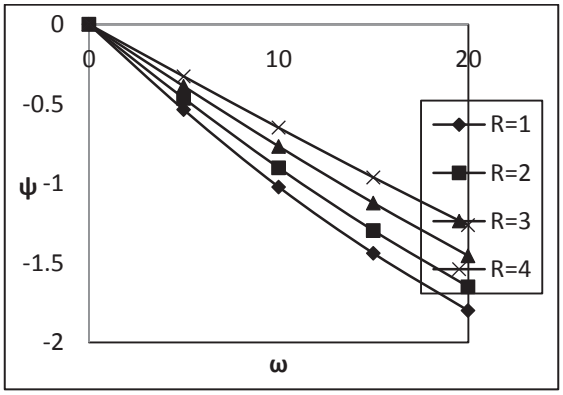

Fig. 25: Phase angle (ψ) of Rate of Heat transfer profile against *Pe* with R=1

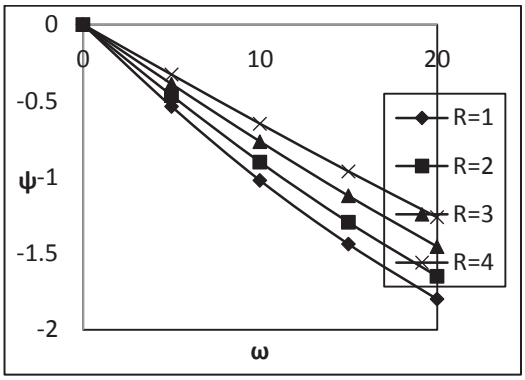

Fig. 26: Phase angle (ψ) of Rate of Heat transfer profile against *R* with *Pe*=0.7

The skin-friction at the plate $z=-1/2$ is obtained in terms of its amplitude $|q|$ and the phase angle ϕ. The amplitude $|q|$ is presented in Table 1. The amplitude $|q|$ increases with increase in Reynolds number Re, pressure gradient *P*, Grashof number *G*r and the Hall parameter *m*. The amplitude $|q|$ increases with increase of permeability of the porous medium *D* for small values of ω ($\omega \le 5$) but decreases for large values of ω ($\omega > 5$). However, the effect of *D* is insignificant for large values of frequency of oscillations ω. The amplitude $|q|$ decreases with increase in the intensity of the magnetic field (Hartmann number *M*). The amplitude $|q|$ increases with increase in Peclet number *Pe* or Radiation parameter *R* for the values of $\omega \le 15$ but decreases for large values of $\omega > 15$. A decrease in $|q|$ is noticed with increasing frequency of oscillations ω. The phase angle ϕ of the skin-friction is presented in Table 2. Since all the values presented in Table 2 are negative, therefore, there is always a phase lag. The phase angle ϕ increases with increasing Reynolds number Re, hall parameter *m*, Peclet number *Pe*, radiation parameter *R* and Grashof number *G*r, while it decreases with increase in permeability of the porous medium *D*, Hartmann number *M* and pressure gradient *P*.

	Re	*M*	*m*	*D*	*Gr*	*Pe*	*R*	*P*	$\omega=5$	$\omega=10$	$\omega=15$	$\omega=20$
I	**1**	**2**	**1**	**1**	**1**	**0.7**	**1**	**10**	0.74175	0.799029	0.622992	0.513032
II	**1.5**	2	1	1	1	0.7	1	10	1.59843	0.879376	0.643293	0.502725
III	**2**	2	1	1	1	0.7	1	10	1.75104	0.90803	0.645668	0.494522
IV	1	**5**	1	1	1	0.7	1	10	0.45904	0.356544	0.339405	0.306986
V	1	**8**	1	1	1	0.7	1	10	0.19977	0.173817	0.179968	0.171313
VI	1	2	**2**	1	1	0.7	1	10	1.50641	0.859331	0.651048	0.530602
VII	1	2	**3**	1	1	0.7	1	10	1.61843	0.900872	0.671557	0.543758
VIII	1	2	1	**2**	1	0.7	1	10	1.23184	0.770207	0.611035	0.506134
IX	1	2	1	**3**	1	0.7	1	10	1.13851	0.739593	0.597566	0.498285
X	1	2	1	1	**3**	0.7	1	10	1.40054	0.863886	0.633323	0.58511
XI	1	2	1	1	**5**	0.7	1	10	1.49245	0.930019	0.65862	0.65719
XII	1	2	1	1	1	**0.9**	1	10	1.31844	0.803141	0.631482	0.507125
XIII	1	2	1	1	1	**1.2**	1	10	1.33554	0.812094	0.638265	0.498909
XIV	1	2	1	1	1	0.7	**5**	10	1.30839	0.850364	0.638895	0.487542
XV	1	2	1	1	1	0.7	**10**	10	1.35168	0.862647	0.642625	0.479671
XVI	1	2	1	1	1	0.7	1	**1**	0.17854	0.021697	0.077568	0.083739
XVII	1	2	1	1	1	0.7	1	**5**	0.68079	0.365671	0.313108	0.274536

Table 1: Amplitude ($|q|$) of Skin friction (τ_L) at lower plate

	Re	*M*	*m*	*D*	*Gr*	*Pe*	*R*	*P*	$\omega=5$	$\omega=10$	$\omega=15$	$\omega=20$
I	**1**	**2**	**1**	**1**	**1**	**0.7**	**1**	**10**	-0.968351	-1.23578	-1.278810	-1.43403
II	**1.5**	2	1	1	1	0.7	1	10	-1.165925	-1.36156	-1.398440	-1.50892
III	**2**	2	1	1	1	0.7	1	10	-1.264428	-1.42965	-1.453360	-1.53187
IV	1	**5**	1	1	1	0.7	1	10	-0.955126	-1.00185	-1.038550	-1.19757

V	1	**8**	1	1	1	0.7	1	10	-0.928135	-0.87620	-0.898628	-1.03272
VI	1	2	**2**	1	1	0.7	1	10	-1.119362	-1.31771	-1.342920	-1.48771
VII	1	2	**3**	1	1	0.7	1	10	-1.132782	-1.33859	-1.361470	-1.50357
VIII	1	2	1	**2**	1	0.7	1	10	-0.949917	-1.16214	-1.222660	-1.38714
IX	1	2	1	**3**	1	0.7	1	10	-0.873865	-1.09131	-1.167210	-1.34025
X	1	2	1	1	**3**	0.7	1	10	-1.157523	-1.27146	-1.321500	-1.45603
XI	1	2	1	1	**5**	0.7	1	10	-1.267641	-1.32527	-1.472756	-1.49762
XII	1	2	1	1	1	**0.9**	1	10	-1.034021	-1.22182	-1.289411	-1.44721
XIII	1	2	1	1	1	**1.2**	1	10	-1.232442	-1.32076	-1.305121	-1.45667
XIV	1	2	1	1	1	0.7	**5**	10	-0.982762	-1.25016	-1.337091	-1.45547
XV	1	2	1	1	1	0.7	**10**	10	-0.991132	-1.27391	-1.353022	-1.47119
XVI	1	2	1	1	1	0.7	1	**1**	-1.484871	-1.74928	-1.865452	-1.69033
XVII	1	2	1	1	1	0.7	1	**5**	-1.097251	-1.25197	-1.359513	-1.53511

Table 2: Phase angle (ϕ) of Skin friction (τ_L) at lower plate

4. Conclusions:

1. The velocity component for primary flow enhances with increasing in Re, *D*, *m*, *Gr*, *Pe* and *P*; and reduces with increasing in the intensity of the magnetic field M (Hartmann number) and Radiation parameter.
2. The velocity component for secondary flow enhances with increasing in *D* and *m*; and reduces with increasing in Re, *M*, *Gr*, *Pe*, *P* and Radiation parameter *R*.
3. The resultant velocity enhances with increasing in Re, *D*, *m* and *P*; and reduces with increasing in *M*, *Gr*, *Pe*, *R* and the frequency of oscillation ω.
4. Temperature reduces with increase in R or Pe while it enhances initially and then gradually reduces with increase in frequency of oscillation ω.
5. The amplitude of rate of heat transfer decreases with the increase of *R* and *Pe*.
6. Phase angle ψ decreases with the increase of *Pe* and increases with increase in *R*. there is only phase log for the values of the frequency of oscillations ω.
7. The amplitude $|q|$ increases with increase in Reynolds number Re, pressure gradient *P*, Grashof number *G*r and the Hall parameter *m*.
8. The amplitude $|q|$ increases with increase of permeability of the porous medium *D* for small values of ω but decreases for large values of ω. However, the effect of *D* is insignificant for large values of frequency of oscillations ω.
9. The amplitude $|q|$ decreases with increase in *M*. The amplitude $|q|$ increases with increase in Peclet number *Pe* or Radiation parameter *R* for the values of ω but decreases for large values of ω.

References:

1. Crammer, K. R. and Pai, S. I. "Magneto Fluid Dynamics for Engineers and Applied Physicists," *McGraw-Hill Book Co. New York*, 1973.
2. Ferraro, V. C. A. and Plumpton, C. "An Introduction to Magneto Fluid Mechanics," *Clarendons Press, Oxford*,1966.
3. B. Radhakrishnan, Existence of Nonlinear Neutral Impulsive; Mathematical Sciences International Research Journal ISSN 2278 – 8697 Vol 3 Issue 1 (2014), Pg 302-306
4. Shercliff, J. A. "A Text Book of Magneto Hydrodynamics," *Pergamon Press Ltd. New York*,1965.
5. Chang, C. and Lundgren, T. S. "Duct flow in Magneto hydro dynamics," *Z. Angew. Math. Phys.*, 12, 1961, pp. 100-114.
6. Yen, T. and Chang, C. "Magneto hydro dynamic Couette flow as affected by wall electrical conductances," *Z. Angew. Math. Phys., (ZAMP),* 15, 1964, pp. 400-407.
7. Ostrach, S. "Combined natural and forced convection Laminar flow and heat transfer of fluids with and without heat sources in channels with linearly varying wall temperatures," *NACATN,* 1954, pp. 31-41.
8. Jain, N. C. and Gupta, P. "Three dimensional free convection Couette flow with transpiration cooling," *Journal of Zhejiang University SCIENCE A,* 7(3), 2006, pp. 340-346.
9. Paul, T., Singh, A.K and Mishra, A.K, "Transient natural convection between two vertical walls filled with a porous material having variable porosity," *Journal of math. Engg. Industry*, Vol.8, No.3, 2001, pp.177-185.

10. Sahin, A. "Three Dimensional channel flows through a porous medium," *Bulletin Calcutta Mathematical Society*, 101(5), 2009, pp. 503.
11. *A.K. Shaikh, R.S.S.Shaikh, M. B. Bhatade ,V.D. Panchal, P. G. Joshi,* Distributed Artificial intelligence and Multi Agent System; Mathematical Sciences International Research Journal ISSN 2278 – 8697 Vol 2 Issue 2 (2013), Pg 408-410
12. Attia, H. A. and Kotb, N. A. "MHD flow between two parallel plates with heat transfer," *ActaMech*, 117, 1996, pp. 215.
13. Soundalgekar, V. M. and Upelkar, A. G. "Hall effects in MHD Couette flow with heat transfer," *IEEE Transactions on Plasma Sci.,* 14(5), 1986, pp. 579-583.
14. *Dr. C. Jaya Subba Reddy, K. Hemavathi,* Assosymmetric Rings With (X, (Xy)2) = 0; Mathematical Sciences International Research Journal ISSN 2278 – 8697 Vol 2 Issue 2 (2013), Pg 400-401
15. Mazumder, B. S., Gupta, A. S. and Datta, N. "Flow and heat transfer in the hydro magnetic Ekman layer on a porous plate with Hall effects," *Int. J. Heat Mass Transfer,* 19, 1976, pp. 523- 527.
16. *V.N.Sendil, M.V.S Naidu,* Statistical Analysis for Technical Compositions of the Soils *P. Ramakrishna Redddy, B.Sarojamma,* ; Mathematical Sciences International Research Journal ISSN 2278 – 8697 Vol 2 Issue 2 (2013), Pg 411-414
17. Mazumder, B. S., Gupta, A. S. and Datta, N. "Hall effects on combined free and forced convective hydro magnetic Flow through a channel," *Int. J. Engng. Sci.,* 14, 1976, pp. 285.
18. Sivaprasad, R., Prasad Rao, D. R. V. and Krishna, D. V. "Hall effects on unsteady MHD free and forced convection flow in a porous rotating channel," *Indian J. Pure Appl. Math.*, 19(7), 1988, pp. 688-696.
19. Singh, K. D. and Rakesh Kumar, "Combined effects of Hall Current and rotation on free convection MHD flow in a Porous channel," *Indian J Pure & Appl. Phys.*, 47, 2009, pp. 617- 623.

L. Hari Krishna/Dept of Mathematics/Annamacharya Institute of Technology and Science/ Rajampet/Kadapa/ Andhra Pradesh/India
M. Veera Krishna/ Department of Mathematics/Rayalaseema University/Kurnool/ Andhra Pradesh/India.